Measurement of Polystyrene Nanospheres Using Excimer Laser Fragmentation Fluorescence Spectroscopy

JONG HYUN CHOI,* CATHERINE P. KOSHLAND, ROBERT F. SAWYER, and DONALD LUCAS

Mechanical Engineering Department, University of California, Berkeley, California 94720 (J.H.C., R.F.S.); School of Public Health, University of California, Berkeley, California 94720 (C.P.K.); and Environmental Energy Technologies Division, Lawrence Berkeley National Laboratory, Berkeley, California 94720 (D.L.)

Monodisperse polystyrene nanospheres with a mean diameter of 102 nm are photofragmented with 193 nm light in N_2 at laser fluences from 1 to 20 J/cm^2. Carbon atom fluorescence at 248 nm from the disintegration of the particles is used as a signature of the polystyrene. The normalized fluorescence signals are self-similar with an exponential decay lifetime of ~10 ns. At fluences above 17 J/cm^2, optical breakdown occurs and a strong continuum emission is generated that lasts significantly longer. A non-dimensional parameter, the photon-to-atom ratio (PAR), is used to interpret the laser-particle interaction energetics. Carbon fluorescence from polystyrene particles is compared with that from soot, and a similarity between the two particles is observed when normalized with PAR. Carbon emission from bulk polystyrene was also measured. Similar emission signals were observed, but the breakdown threshold of the surface is significantly lower at 0.2 J/cm^2.

Index Headings: **Nanosphere; Nanoparticle; Photofragmentation; Fluorescence; Disintegration; Breakdown; Plasma; Excimer laser fragmentation fluorescence spectroscopy; ELFFS.**

INTRODUCTION

Combustion processes are a dominant source of small particles in the atmosphere, and these particles adversely affect environmental and human health.[1] Evidence suggests that many adverse impacts may be associated with nanoscale particles. Nanoparticles may be more effective in transporting toxic materials during exposure as a result of their high surface area per unit volume.[2] The unique properties of many nanoscale particles, while posing potential risks, are the assets leading to applications in drug delivery,[3] bio-molecule detection,[4] and microelectronics,[5] to name a few. The widespread potential as well as concerns make it desirable to develop accurate analytical techniques to characterize basic particle properties, including chemical composition, size, morphology, and concentration.

Various *in situ,* real-time spectroscopic methods have been employed to monitor airborne nanoparticles. Laser-induced incandescence (LII) utilizes visible/infrared (IR) laser beams with intensities lower than 10^7 W/cm^2 to heat the particles without significant vaporization.[6] The broadband incandescence is used to deduce information on primary particle size and volume fraction. Laser-induced breakdown spectroscopy (LIBS) employs higher intensity visible/IR lasers to create a plasma, thermally disintegrate the particles, and measure atomic emission in the plume as the gases cool.[7] Direct ablation with ultraviolet (UV) lasers is used to generate neutral atoms, molecules, and ions for chemical analysis, such as aerosol time-of-flight mass spectrometry (ATOFMS).[8] Excimer laser fragmentation fluorescence spectroscopy (ELFFS) uses mildly focused UV light to photolytically decompose non-fluorescing large molecules or particles into smaller, fluorescent species without significantly heating the particles/molecules or creating a plasma. The fluorescence is measured as a signature of the parent molecules or particles, providing information on the chemical composition and concentration. We and other researchers previously used ELFFS to measure combustion-generated species,[9–11] particles,[12–15] and toxic metals in soil.[16] The interaction of UV photons with particles was also used to disintegrate the particles and produce nanoparticles with a controlled size and morphology.[17–20] However, questions with regard to the extent of particle disintegration and the behavior of the ejected species that influence the measured emission have not been fully answered.

Laser interactions with combustion-generated soot, the most commonly encountered atmospheric particles, are complex; the interaction strongly depends on the wavelength and energy of the light, the particle size, and the chemical composition. In addition, soot particles are fractal agglomerates of primary particles. To simplify the study of the basic behavior of nanoparticles with 193 nm light, we irradiate monodisperse polystyrene nanospheres with 193 nm photons. Unlike soot, polystyrene particles possess a uniform size, are spherical, and have well-characterized material and optical properties. A better understanding of the nanoparticle interaction with UV light, which has features distinct from gas or solid interactions, helps to improve not only laser-based measurements of soot and other aerosol particles, but also novel nanoparticle production techniques using UV light.

The specific aims of the present study are to (1) analyze the characteristics of carbon atom fluorescence produced by 193 nm laser irradiation of polystyrene nanospheres, (2) measure the emission formed by the optical breakdown of small particles, (3) develop a parameter (the photon/atom ratio or PAR) to estimate the extent of particle disintegration, and (4) assess how laser-particle interactions differ from laser interactions with a gas or a bulk solid.

EXPERIMENTAL

Nearly monodisperse polystyrene $(C_8H_8)_n$ nanospheres in water (Duke Scientific) have a size distribution of 102 ± 3 nm. Nitrogen gas at 6 standard liters per minute

Received 23 March 2005; accepted 8 July 2005.

* Author to whom correspondence should be sent. E-mail: jhyunc@me.berkeley.edu.

0003-7028/05/5910-1203$2.00/0

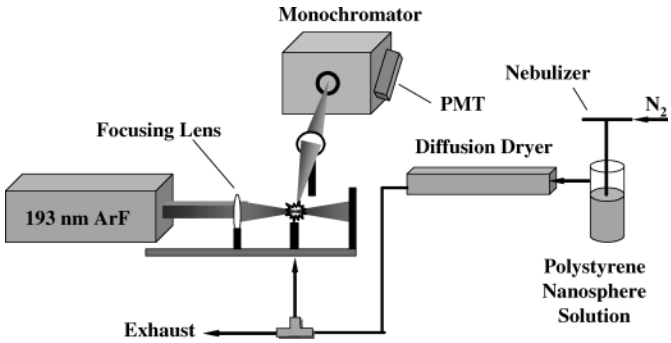

FIG. 1. Schematic of the laser and optical emission measurement system.

(slpm) is supplied to a 3-jet Collision nebulizer (BGI, CN-24), generating droplets from the polystyrene solution diluted with distilled water (Fig. 1). The droplets pass through a diffusion dryer (TSI 3062) that removes water from the particle-laden flow. The polystyrene nanospheres in the N_2 stream (number concentration = 1.6×10^5 cm^{-3}) are introduced into the laser interrogation region at 0.3 slpm. Some of the nebulized particles agglomerate, but size distribution and morphology measurements with a scanning mobility particle sizer and a transmission electron microscope reveal that individual nanospheres dominate the distribution. For the solid measurements, a 1.5 mm thick polystyrene sheet was obtained from Professional Plastics. A 3×3 cm^2 piece of the sheet is irradiated normal to the incident light in an N_2 environment.

An ArF excimer laser (Lambda Physik, LPX 210i) generates 193 nm pulses with a duration of 20 ns. According to the manufacturer, the spatial profile of the laser beam is flat-top across the width and Gaussian across the height. The laser beam is focused by either a 3.8 cm diameter, 25 cm focal length or a 2 cm diameter, 6 cm focal length UV-grade fused silica lens (CVI Corp.). The laser energy is measured with a Gentec joulemeter (ED-500+). The beam footprint is determined by placing a paper in the laser interrogation region and measuring the size of the hole made by the focused laser pulses using a microscope. The fluence is varied by changing the laser charging voltage. The fluences from 0.1 to 20 J/cm^2 are used at repetition rates of 1 and 4 Hz. The residence time of the particles in the focal volume ranges from 20 to 70 ms, so the flow field is frozen compared to the laser–particle interaction timescale (~20 ns). Hundreds to several thousand nanospheres interact with a single laser pulse. The optical emission is collected at a right angle by a 5 cm diameter bi-convex collection lens and is transferred to a GCA/McPherson 0.3 m scanning monochromator with a Hamamatsu R928 photomultiplier tube (PMT). The PMT signal is recorded on a LeCroy LT342 digital oscilloscope without any time gating. The slit width of the monochromator is 0.4 mm, corresponding to a 1.1 nm spectral bandwidth.

RESULTS AND DISCUSSION

Figure 2 presents the time-resolved atomic carbon emissions (248 nm) from polystyrene nanospheres in N_2 for laser fluences from 2 to 20 J/cm^2. The signals are

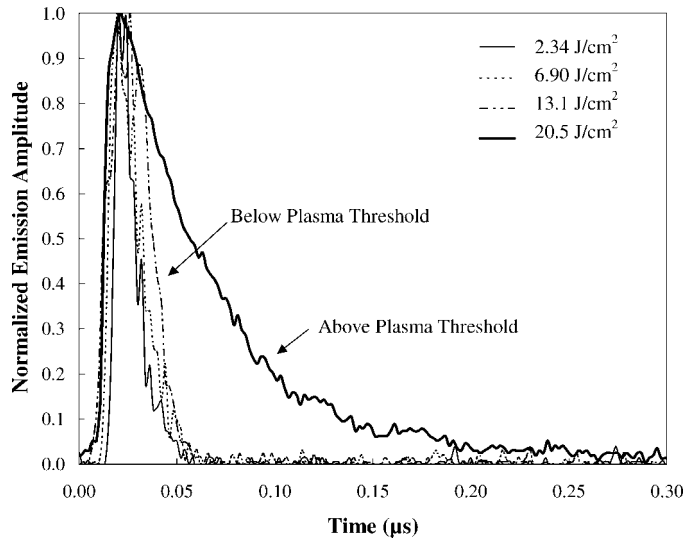

FIG. 2. The time characteristics of the normalized optical emissions of carbon atoms at 248 nm from polystyrene nanospheres in a N_2 stream as a function of laser fluence at 4 Hz. Optical breakdown occurs at approximately 17 J/cm^2. Below the breakdown threshold, the fluorescence signals are self-similar with a decay lifetime of ~10 ns. Once breakdown occurs, the emission become continuous and the signal lasts significantly longer.

normalized in magnitude and shifted in time to a common scale as the different laser conditions affect the signal magnitude and time at which lasing actually occurs compared to the trigger pulse. The 193 nm photons convert a fraction of the particles into gas-phase atoms, molecules, and ions, producing some carbon atoms in an electronically excited state ($^1P_1^0 \leftarrow {}^1D_2$) through a multiphoton process. The C($^1P_1^0$) atoms subsequently fluoresce to the $^1S_0$ ground state at 248 nm. While photochemical pathways to produce C($^1D_2$) from the polystyrene particles are very complex, the processes from various gas-phase molecules are relatively well understood.[11,21] The resonance between the laser output and the electronic excitation of carbon atoms makes the measurement more sensitive. Previous measurements of 248 nm fluorescence from carbon-based particles showed that the detection limit of carbon atoms using this ELFFS system is sub-ppb.[12] The C atoms in the $^1P_1^0$ state also depopulate due to collisional quenching. The collision-free lifetime in the excited state is approximately 29 ns.[22] Exponential curve fitting of the signals in the figure shows that the decay of the 248 nm emission at fluences from 2 to 13 J/cm^2 is approximately 10 ns. In this range, the normalized emissions are self-similar.

Direct photochemical bond breaking is the dominant mechanism in the laser–particle interactions. We observe no broadband incandescence associated with particle heating using 193 nm light, while the same nanoparticles irradiated by 532 nm pulses at similar fluences emit incandescence. Other researchers observed that ArF laser irradiation of a solid polymer surface produced fragments ranging from diatomics to high molecular weight products and concluded that thermal effects were insignificant.[23,24] A mass spectrometry study in vacuum showed that the major product from the photochemical decomposition of a bulk polystyrene surface is neutral styrene monomers (C_8H_8).[25] In this work we do not observe other

lines, such as CH at 431 nm ($A^2\Delta \rightarrow X^2\Pi$) and C_2 at 468 nm ($d^3\Pi_g \rightarrow a^3\Pi_u$), which were observed with diesel soot[12] and hydrocarbon-adsorbed soot particles at similar laser conditions in our laboratory.

At 20.5 J/cm^2, the emission lasts longer with an exponential decay lifetime of approximately 70 ns, and the peak of the signal is an order of magnitude larger than those at fluences from 2 to 13 J/cm^2, owing to plasma formation. Recombination of species in a high-temperature (>10 000 K) plasma gas takes place as the hot gas cools. Therefore, emission from the plasma lasts significantly longer than atomic fluorescence in the absence of optical breakdown. The mechanisms that initiate breakdown have been discussed previously.[26–29] As laser fluence increases, more atoms, molecules, ions, and electrons are ejected, and continuum absorption of intense UV photons by the electrons leads to cascade collision ionization and optical breakdown. Once optical breakdown occurs, a strong visible and audible emission is generated. The breakdown threshold in our system is approximately 17 J/cm^2. LIBS generates this type of signal with laser intensity greater than 10^9 W/cm^2 and monitors atomic emission lines with time gating. ELFFS typically utilizes laser intensities low enough to avoid optical breakdown ($10^7 \sim 10^9$ W/cm^2) and measures the fluorescence peaks of the emitting species fragmented from the irradiated particles where the temperature change is negligible.

The background signals are also measured at 255 nm (not shown), where there is no known transition, and similar phenomena are observed. The background signal at fluences from 2 to 13 J/cm^2 lasts approximately 10 ns. The signal is 3 to 7 times smaller than carbon fluorescence at 248 nm. At 20.5 J/cm^2 where the plasma is formed, the background signal is almost identical to the emission at 248 nm. This strong background emission is observed over a wide range of wavelengths. ELFFS benefits from an increased signal-to-noise ratio without time gating since there is no intense continuum emission that interferes with analyte signals.

The 100 shot average fluorescence at 248 nm with the averaged background signal at 255 nm subtracted is shown as a function of laser fluence in Fig. 3a. These results are compared to combustion-generated soot results from our previous study.[15] The soot particles, generated by a well-controlled non-premixed flame, are composed of mainly elemental carbon as confirmed by ELFFS and EC/OC measurements. The particles have a polydisperse size distribution with a mean diameter of 280 nm and a number concentration of 9.2×10^5 cm^{-3}. The soot is an agglomerate composed of nearly 40 nm primary particles with a fractal dimension near 1.8. The fluorescence signals from these two kinds of particles are normalized in magnitude since soot particles have a much higher concentration, yielding stronger signals.

The fluorescence signal from polystyrene increases linearly with laser fluence from 1 to 3 J/cm^2. The signal saturates above 6 J/cm^2 and remains constant until breakdown occurs. This type of fluorescence saturation at higher fluence was also observed with gas-phase molecules, such as NH fragmented from NH_3,[9] and makes ELFFS more robust for quantitative chemical analysis as shot-to-shot variations in the laser energy do not significantly affect the emission signals. In this study we did not determine the lower limit of laser fluence necessary to produce detectable carbon fluorescence from the nanospheres. However, we observed that laser irradiation of different particles including soot,[20] NaCl,[18] polystyrene, and gold at fluences below 0.3 J/cm^2 partially disintegrated the particles and produced smaller particles with an order of magnitude higher concentration. The low fluence photolysis generates gas-phase species that subsequently nucleate to form a new mode of particles.

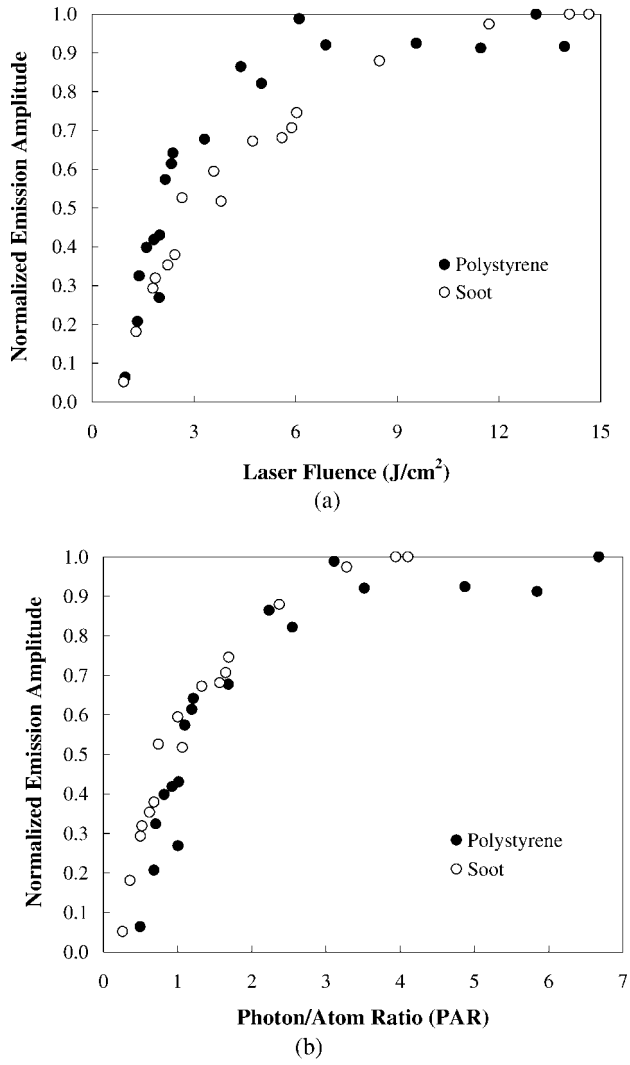

FIG. 3. The 100 shot average carbon fluorescence from polystyrene and soot particles for various laser fluences and photon/atom ratios at 4 Hz. The fluorescence by ELFFS shows linear, intermediate, and saturation regimes. (**a**) Normalized fluorescence from the particles as a function of laser fluence. (**b**) Normalized fluorescence from the particles as a function of PAR.

The carbon signals from soot also have linear, intermediate, and saturation regimes. In the soot system, however, the fluorescence increases at a slower rate; the linear regime ends at approximately 6 J/cm^2 and the saturation begins around 12 J/cm^2 owing to different chemical composition and larger size, indicating that the extent of disintegration of these two particles is different.

We use a non-dimensional parameter, called the photon-to-atom ratio or PAR, to interpret these data. PAR is the ratio of the number of absorbed photons to the num-

ber of atoms in the particle and has been discussed previously.[15,18,20] The laser fluence that is conventionally used to describe the laser energy density is effective for homogeneous target media such as pure gases or bulk solids, but nanoparticles suspended in a gas are discrete objects in the laser probe volume. The photon energy density for these particles can be better described by considering the energy balance for each particle. For laser–particle interactions, the photon/atom ratio is more relevant than the fluence, because the total number of atoms is a function of particle volume ($\sim d^3$) while the number of photons striking a particle depends on the cross-sectional area ($\sim d^2$). For photons with the same energy as the average bond energy in a particle, the PAR must be unity or higher for complete fragmentation of the particle. The number of photons striking the particles is calculated using the laser fluence and the cross-sectional area of the particles, while the number of atoms is obtained with the particle density and volume. The PAR concept can be expanded by accounting for the absorption efficiency of the particle material and incident wavelength. The absorption process of incident photons depends on the particle material, diameter, and wavelength. Here, the PAR values are corrected for the 57% absorption of 193 nm light by 102 nm polystyrene nanospheres using Mie theory[30] with a complex refractive index of 1.6–1.23i.[31]

The normalized fluorescence signals from polystyrene and soot are presented as a function of PAR in Fig. 3b. These two signals appear similar; both polystyrene and soot have a linear regime up to a PAR = 1.5 and saturate above a PAR = 3. The good agreement in the fluorescence signals, regardless of particle material, diameter, shape, dispersion in size, and concentration, indicates that PAR can be an effective tool for understanding laser–particle interactions, and can be used to assess the amount of particle disintegration. When the 193 nm irradiation of soot or carbon-based polymer particles meets the condition of PAR = 3 or higher, the particles can be considered to be disintegrated into atomic species. Note that the PAR is corrected for absorption efficiency of 193 nm photons by particles. If the irradiated particle material were not to efficiently absorb 193 nm light, the saturation condition would not be achieved and a majority of particles would not be disintegrated. The saturation near PAR = 3 also suggests that the photofragmentation process is not perfectly efficient; at least 2 photons are necessary for the liberation and electronic excitation of an atom. However, 193 nm laser photolysis is much more efficient in particle disintegration than direct laser ablation methods or LIBS with nanosecond laser pulses that use orders of magnitude more photons to create a plasma and thermally disintegrate the particles. Optical breakdown occurs approximately at a PAR = 8.7 (17 J/cm^2), implying that a plasma is formed when approximately 9 photons strike each atom in the nanospheres. Note that in this work the PAR is used as a comparative parameter for different particle composition, size, morphology, and concentration, and there are assumptions and approximations that the particles are evenly distributed in the laser probe volume and the laser energy for the PAR calculation is temporally and spatially averaged.

Figure 4 shows the time-resolved carbon emissions from the surface of the polystyrene sheet. The sheet is manually translated in the vertical direction so that each shot fragments a fresh surface. The characteristic emission from the bulk solid is analogous to that from nanospheres. The self-similar emissions at 0.08 and 0.12 J/cm^2 have an exponential decay time of approximately 10 ns. The magnitude of the signal increases with the laser fluence from 0.08 to 0.2 J/cm^2. At 0.2 J/cm^2, optical breakdown occurs, creating intense white light, and the signal lasts longer. Then, the lifetime of the emission further increases with fluence as the plasma plume grows. The decay lifetime of the signal at 0.3 J/cm^2 is longer than 100 ns. Once the plasma is formed, the signal magnitude remains at approximately 60 mV, similar to the value for the nanospheres, even at higher laser fluences. The saturation of the signal above the plasma threshold is likely due to the probe volume being filled with the hot plasma gas. A similar phenomenon is observed with the background emissions at 255 nm from the bulk surface (not shown); the signals have a decay time of ~10 ns at 0.08 and 0.12 J/cm^2, which increases with the laser fluence as the plasma plume develops. When the plasma forms, the background signal becomes identical to the carbon signal at 248 nm. The background, however, increases faster at lower fluences, resulting in a decrease of the signal-to-noise ratio. Thus, low laser fluences should be used for ELFFS detection of a bulk material to maintain a high signal-to-noise ratio.

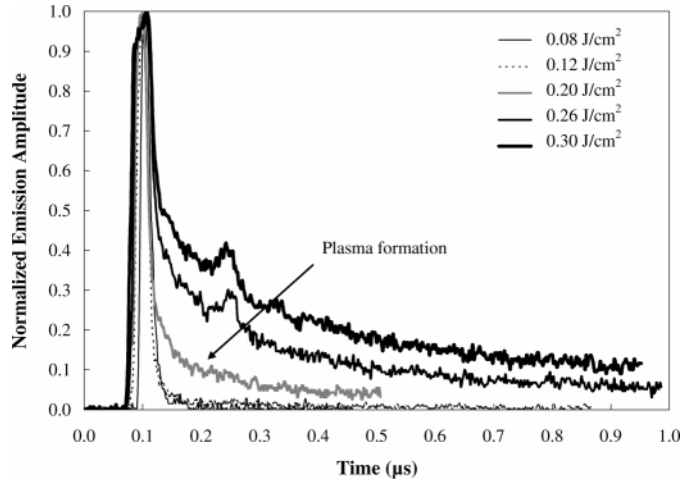

FIG. 4. The time characteristics of the normalized emissions of carbon atoms from a solid polystyrene surface. The laser fluences range from 0.08 to 0.3 J/cm^2 at 1 Hz. The signals are similar to those from nanospheres. The plasma appears approximately at 0.2 J/cm^2.

The ELFFS measurements of Pb at 405.8 nm from a solid $Pb(NO_3)_2$ surface in our previous study produced similar results.[16] The Pb emission increases with fluence and saturates when the plasma forms. The emission produced by optical breakdown lasts significantly longer and the decay lifetime further increases with the fluence. However, the breakdown threshold for $Pb(NO_3)_2$ was approximately 2 J/cm^2, which is a factor of 10 higher than that for polystyrene. Lencioni[32] showed that the breakdown threshold for bulk surface could vary more than an order of magnitude for different materials. Feldmann et al.[25] also observed that 13 ns pulses of 193 nm light from 0.015 to 0.05 J/cm^2 photochemically decomposed a solid polystyrene surface with no plasma formed. The 193 nm

laser photolysis of other polymer surfaces, such as poly(methyl methacrylate) (PMMA),[23] produced detectable species at fluences as low as 0.014 J/cm^2 and significant photodecomposition starting at 0.07 J/cm^2. The photochemical cleavage of PMMA continued up to 0.5 J/cm^2, likely due to the lower absorption coefficient of the material (2×10^3 cm^{-1}) compared to polystyrene (8×10^5 cm^{-1}).

The breakdown threshold of bulk polystyrene (0.2 J/cm^2 or 10^7 W/cm^2) is two orders of magnitude lower than the threshold for the gas–particle mixture, an indication that small particles interact differently with lasers than pure gases or bulk solids. The presence of particles in a gas reduces the gas breakdown threshold. In this study, the plasma in the particle–gas mixture is formed near 17 J/cm^2, while the optical breakdown in pure N_2 is not observed even at 20 J/cm^2 (10^9 W/cm^2). Pure nitrogen has a very high breakdown threshold, 5×10^{11} W/cm^2 at 350 nm.[33] Even taking into account the decreasing trend of the threshold with wavelength in the UV/visible range,[34,35] the plasma threshold of pure N_2 gas would be far above 10^9 W/cm^2. Pinnick et al.[27] also reported that the breakdown threshold of gas–particle mixtures is more than two orders of magnitude lower than that of the pure gas and decreases with light in the UV/visible range. When compared with carbon-containing gases, the breakdown thresholds of polystyrene particles in N_2 is 50 times lower; e.g., the thresholds of CO and CO_2 at 1 atm by 193 nm laser irradiation are 2×10^{10} and 7×10^{10} W/cm^2, respectively.[28]

The gas breakdown threshold induced by the particles is also a function of the particle diameter. As shown by Smith[36] and Lencioni,[32] the threshold monotonically decreases with increasing particle diameter. For instance, air breakdown by a 10.6 μm laser occurs near 4×10^9 W/cm^2 in the presence of 300 nm carbon particles, while 3 μm particles decrease the threshold to 3×10^8 W/cm^2. An inverse dependence of breakdown threshold on particle diameter is observed up to 10 μm. As the particles become larger, the threshold approaches the value corresponding to the laser–bulk solid interaction, e.g., 10^7 W/cm^2 for solid carbon. Depending on the particle diameter, material, and wavelength, the breakdown threshold induced by the particles is higher than the threshold from laser–solid interaction by a factor of 10 to 100, similar to what we observe with the polystyrene nanoparticles and solid. On the other hand, the threshold approaches that of a pure gas as the particles become smaller. Another point to consider in particle-induced breakdown is that the threshold tends to decrease with increasing particle concentration. The threshold is determined by the largest particle in the focal volume, and larger particles likely exist at higher concentrations due to agglomeration.[32] In the breakdown threshold measurements, accurate determination of the particle size is the most difficult task and the main source of experimental uncertainty. Note that the absorption process, the particle size, and the chemical composition determine the mode of photodecomposition of the particle surface and the behavior of the ejected species. Therefore, the photon-to-atom ratio can be useful in understanding particle disintegration by UV photons and gives an insight into laser–particle interactions, which are different than the interactions with gases or solids.

CONCLUSION

Polystyrene nanospheres in N_2 are measured with ELFFS to study the photochemical interactions between the nanoparticles and 193 nm light. The characteristic carbon emissions from the particles are analyzed and compared to the signals produced when a plasma is formed. In ELFFS, the emissions from the nanospheres are self-similar and have an exponential decay lifetime of ~10 ns. Once a plasma is formed by intense UV irradiation, a strong continuum emission is generated and the signal lasts significantly longer. While fluorescence signals from polystyrene and soot particles have linear, intermediate, and saturation regimes, the signals have different slopes with laser fluence, indicating that the extent of disintegration of the two particles is different. When normalized using the photon/atom ratio, a similarity in the signals from the two particle types is established independent of different particle properties and laser conditions, suggesting that the extent of particle disintegration can be estimated with PAR. The PAR for complete particle disintegration and electronic excitation of liberated carbon atoms is approximately 3. The plasma threshold of polystyrene particles in N_2 is found to be 17 J/cm^2 while the threshold for a bulk polystyrene surface decreases to 0.2 J/cm^2, which implies that laser interactions with small particles are different than with a bulk solid.

ACKNOWLEDGMENTS

We thank Dr. Thomas Kirchstetter for providing EC/OC measurements. This work was supported by the Environmental Health Sciences Superfund Basic Research Program (Grant Number P42ESO47050-01) from the National Institute of Environmental Health Sciences, NIH, with funding provided by the EPA.

1. C. P. Koshland and S. L. Fisher, ''Diagnostic Requirements for Toxic Emission Control,'' in *Applied Combustion Diagnostics*, K. Kohse-Hoinghaus and J. B. Jeffries, Eds. (Taylor and Francis, New York, 2002), Chap. 24, p. 606.
2. M. D. Cheng, B. Malone, and J. M. E. Storey, Chemosphere **53,** 237 (2003).
3. F. Yu, Y. Liu, and R. Zhuo, J. Appl. Polym. Sci. **91,** 2594 (2004).
4. J. M. Nam, C. S. Thaxton, and C. A. Mirkin, Science (Washington, D.C.) **301,** 1884 (2003).
5. H. Htoon, J. A. Hollingsworth, A. V. Malko, R. Dickerson, and V. I. Klimov, Appl. Phys. Lett. **82,** 4776 (2003).
6. H. A. Michelsen, J. Chem. Phys. **118,** 7012 (2003).
7. D. W. Hahn and M. M. Lunden, Aerosol Sci. Technol. **33,** 30 (2000).
8. D. T. Suess and K. A. Prather, Chem. Rev. **99,** 3007 (1999).
9. S. G. Buckley, C. J. Damm, W. M. Vitovec, L. A. Sgro, R. F. Sawyer, C. P. Koshland, and D. Lucas, Appl. Opt. **37,** 8382 (1998).
10. C. S. McEnally, D. Lucas, C. P. Koshland, and R. F. Sawyer, Appl. Opt. **33,** 3977 (1994).
11. R. C. Sausa, A. J. Alfano, and A. W. Miziolek, Appl. Opt. **26,** 3588 (1987).
12. C. J. Damm, D. Lucas, R. F. Sawyer, and C. P. Koshland, in *29th Symposium (International) on Combustion* (The Combustion Institute, 2002).
13. M. H. Nunez, P. Cavalli, G. A. Petrucci, and N. Omenetto, Appl. Spectrosc. **54,** 1805 (2000).
14. M. H. Nunez and N. Omenetto, Appl. Spectrosc. **55,** 809 (2001).
15. C. B. Stipe, D. Lucas, C. P. Koshland, and R. F. Sawyer, ''Soot Particle Disintegration and Detection Using Two Laser ELFFS,'' Appl. Opt., paper accepted (2005).
16. J. H. Choi, C. J. Damm, N. J. O'Donovan, R. F. Sawyer, C. P. Koshland, and D. Lucas, Appl. Spectrosc. **59,** 258 (2005).
17. H. Cai, N. Chauhary, J. Lee, M. F. Becker, J. R. Brock, and J. W. Keto, J. Aerosol Sci. **29,** 627 (1998).

18. J. H. Choi, C. B. Stipe, C. P. Koshland, R. F. Sawyer, and D. Lucas, J. Appl. Phys. **97,** 124315 (2005).
19. P. V. Kamat, M. Flumiani, and G. V. Hartland, J. Phys. Chem. B **102,** 3123 (1998).
20. C. B. Stipe, J. H. Choi, D. Lucas, C. P. Koshland, and R. F. Sawyer, J. Nanopart. Res. **6,** 467 (2004).
21. J. Bokor, J. Zavelovich, and C. K. Rhodes, J. Chem. Phys. **72,** 965 (1980).
22. http://physics.nist.gov/cgi-bin/AtData/lines_form.
23. R. Srinivasan, B. Braren, D. E. Seeger, and R. W. Dreyfus, Macromol. **19,** 916 (1986).
24. E. Sutcliffe and R. Srinivasan, J. Appl. Phys. **60,** 3315 (1986).
25. D. Feldmann, J. Kutzner, J. Laukemper, S. MacRobert, and K. H. Welge, Appl. Phys. B **44,** 81 (1987).
26. P. Chylek, M. A. Jarzembski, V. Srivastava, R. G. Pinnick, J. D. Pendleton, and J. P. Cruncleton, Appl. Opt. **26,** 760 (1987).
27. R. G. Pinnick, P. Chylek, M. A. Jarzembski, E. Creegan, V. Srivastava, G. Fernandez, J. D. Pendleton, and A. Biswas, Appl. Opt. **27,** 987 (1988).
28. J. B. Simeonsson and A. W. Miziolek, Appl. Opt. **32,** 939 (1993).
29. D. Smith and R. Brown, J. Appl. Phys. **46,** 1146 (1975).
30. C. F. Bohren and D. R. Huffman, *Absorption and Scattering of Light by Small Particles* (Wiley Interscience, New York, 1983).
31. J. Meyer, J. Kutzner, D. Feldmann, and K. H. Welge, Appl. Phys. B **45,** 7 (1988).
32. D. E. Lencioni, Appl. Phys. Lett. **23,** 12 (1973).
33. D. I. Rosen and G. Weyl, J. Phys. D: Appl. Phys. **20,** 1264 (1987).
34. A. J. Alcock, K. Kato, and M. C. Richardson, Opt. Commun. **6,** 342 (1972).
35. H. T. Buscher, R. G. Tomlinson, and E. K. Damon, Phys. Rev. Lett. **15,** 847 (1965).
36. D. Smith, J. Appl. Phys. **48,** 2217 (1977).